J. Earth Syst. Sci. (2019)128:101
https://doi.org/10.1007/s12040-019-1124-7

Illite crystallinity index from the Mesoproterozoic sedimentary cover of the Kaladgi basin, southwestern India: Implications on crustal depths of subsidence and deformation

Mrinal Kanti Mukherjee[1,*], Kunal Modak[1] and Jiten Ghosh[2]

[1] *Department of Applied Geology, Indian Institute of Technology (Indian School of Mines), Dhanbad 826004, Jharkhand, India.*
[2] *Advanced Mechanical and Material Characterization Division, CSIR-Central Glass and Ceramics Research Institute, Jadavpur, Kolkata 700032, India.*
**Corresponding author. e-mail: mrinal_km67@yahoo.co.in*

MS received 20 January 2018; revised 15 July 2018; accepted 18 October 2018

The grade of metamorphism and thermal maturity of the Mesoproterozoic Bagalkot Group in the Kaladgi basin of southwestern India has been determined using the illite crystallinity (IC) index. IC index was determined from the argillite samples of four stratigraphic levels viz., Ramdurg Formation (basal unit), Yargatti Formation (intermediate lower unit), Yadahalli Formation (intermediate upper unit) and Hoskatti formation (upper unit). IC index (Kubler equivalent) values range between 0.54°$\Delta 2\theta$ and 0.24°$\Delta 2\theta$ (in a set of 37 samples) and indicate a deep diagenetic to high anchizone metamorphic grade within a temperature range of ∼180 to 300°C. The Mesoproterozoic sedimentary cover of the Kaladgi basin is deformed due to southerly directed gravity gliding of the cover over the basement. The general variation of the IC index along and across the basin as indicated by the distribution of IC index values and isocryst contour patterns is due to the combined effect of deformation and variable subsidence of the Mesoproterozoic cover of the basin. Considering an average Mesoproterozoic geothermal gradient of 35°C/km, the crustal depth of deformation and/or subsidence of the Mesoproterozoic cover up to the sample point is estimated to vary between 5.14 and 8.57 km.

Keywords. Kaladgi basin; illite crystallinity; deformation; subsidence.

1. Introduction

The illite crystallinity (IC) index is a commonly used parameter for describing low-grade metamorphism of pelitic rocks (e.g., Kübler 1967; Kisch 1983; Frey 1987; Merriman and Peacor 1999; Kübler and Jaboyedoff 2000; Jaboyedoff et al. 2001). Illite is a phyllosilicate consisting of 'packet' of 10-Å thick sheets, which in turn are made up of tetrahedral and octahedral aluminosilicate layers separated by interlayer potassium cations (e.g., Moore and Reynolds 1997). The IC index is the numerical expression of the basal (001) 10-Å illite X-ray diffraction (XRD) peak at one-half of its height [known as field width at half maxima (FWHM)] and is typically reported in units of °$\Delta 2\theta$, where $\Delta 2\theta$ is the XRD angle (Kübler 1967; Kübler and Jaboyedoff 2000). The 10-Å peak of illite (001) in XRD gradually sharpens as metamorphic grade increases. The IC index

Published online: 03 April 2019

was introduced by Kübler (1967) and is used to define diagenetic and low-grade metamorphic zones in pelitic rocks. On the basis of IC index, these zones are classified as diagenetic ($IC > 1^\circ\Delta 2\theta$), anchizone ($IC 0.42^\circ\Delta 2\theta - 0.25^\circ\Delta 2\theta$) and epizone ($IC < 0.25^\circ\Delta 2\theta$). IC index is a commonly used method to determine metamorphic zones and is also used as a common geothermometer because of ease of measurements, despite arguments that IC cannot be used as an accurate geothermometer (Essene and Peacor 1995). Abundance of illite in most mudrocks in sedimentary basins makes it possible to measure the thermal maturity in a basin-wide scale and to detect the potential heat sources. IC is especially useful in reconstructing the structural and metamorphic history in very low- to low-grade metamorphic rocks (e.g., Frey et al. 1980; Roberts and Merriman 1985; Frey 1988; Gutierrez-Alonso and Nieto 1996; Roberts et al. 1996; Warr et al. 1996; Lee and Ko 1997; Mukherjee 2003; Merriman 2006; Ruiz et al. 2008; Hara and Kurihara 2010; Verdel et al. 2011; Fitz-Díaz et al. 2014; Fukuchi et al. 2014). In addition, the spatial variation in sediment thickness (e.g., Awan and Woodcock 1991) and the existence of concealed plutons (e.g., Roberts et al. 1990; Lee and Lee 2001) can be examined on the basis of IC variation.

In this paper, the determination, distribution and variation of IC index are documented from the deformed Mesoproterozoic sedimentary cover in an intracratonic basin in southwestern India. IC index values are further used to define low-grade metamorphic zones of the rocks and estimate the crustal depth of subsidence and deformation.

2. Geological background

The east–west trending Kaladgi basin is located in the northern part of the Dharwar Craton, and it is spread over an area of ~8300 km^2 (Jayaprakash et al. 1987, 2007). The basin has an irregular elliptical outline and extends over a length of 250 km with a great part concealed beneath the vast spread basaltic lava flows of the Deccan Traps of Upper Cretaceous to Lower Eocene age (Wensink and Klootwijk 1970; Mani 1974) in the north and in the west (figure 1). In the north, the outcrops occur as inliers within the Deccan Traps near Jamkhandi, and similar strata may extend further north beneath the Deccan Trap flows. The Archaean basement of the basin is a part of western Dharwar Craton and constitutes an assemblage of Peninsular Gneissic Complex (PGC) occurring to the south of the basin, granites (Closepet granite) that occur to the north, central and southeastern parts of the basin, and the Hungund schist belt (HSB) that occupies the eastern part of the basin (Jayaprakash et al. 1987; figures 1, 2).

The basin covers rock successions comprising three sequences bounded by regional unconformities (table 1). The lowermost Lokapur Subgroup is the thickest sequence (~3.1 km) that occurs throughout the basin. The Simikeri Subgroup is confined to the east-central parts of the basin and is separated from the underlying Lokapur Subgroup by a disconformity. The Lokapur and Simikeri Subgroups are of Mesoproterozoic age as determined from the stromatolite biostratigraphy (cf. Pillai 1997; Kulkarni and Borkar 1999) and carbon/strontium isotope data from carbonates and shales (cf. Padmakumari et al. 1998; Rao et al. 1999) and Late Palaeoproterozoic to early Mesoproterozoic age by Sharma and Pandey (2012). Patil et al. (2018) generated 40Ar/39Ar date of 1154 ± 4 Ma from a mafic dyke that is intrusive along an axial plane of a fold in the Bagalkot Group, indicating a Mesoproterozoic age of the deformation. The Lokapur and Simikeri Subgroups constitute the Bagalkot Group (table 1). The younger Badami Group of Neoproterozoic age is separated from the underlying Simikeri Group by an angular unconformity. The distribution of the Badami Group of rocks is restricted to the southern and western parts of the basin. In the southern parts of the basin, the Badami Group unconformably overlies the Lokapur Subgroup as well as the basement rocks of the Dharwar Craton (figure 1). The general lithostratigraphy of the basin is outlined in table 1.

The Lokapur and Simikeri Subgroups, in general, are composed of cherts and coarse siliciclastics that include granular arkose, quartz arenites and lensoidal bands of polymictic conglomerates along the basin margin that grades gradually through argillites to carbonates towards the interior basin (Kale and Phansalkar 1991; Pillai and Kale 2011). The total thicknesses of the Mesoproterozoic sediment cover of the Kaladgi basin is 4234 m. The Mesoproterozoic cover of the Kaladgi basin is reported to have been deformed into elongated regional dome-and-basin patterns that are oriented from WNW–ESE to E–W. Deformation is relatively intense in the south-central sectors of the basin and mild to almost no deformation in the northern margins (Jayaprakash et al. 1987;

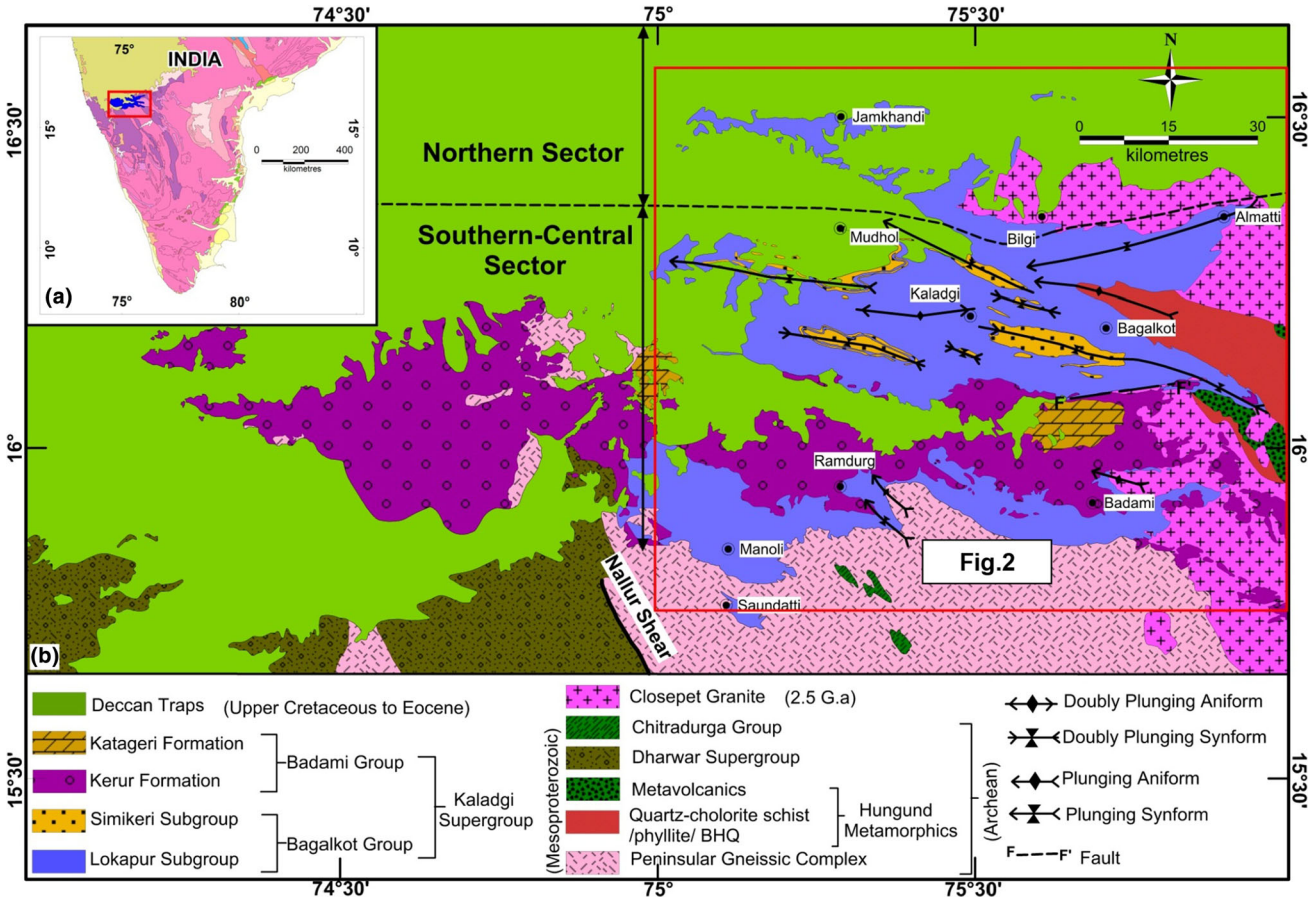

Figure 1. (**a**) Inset shows the position of Kaladgi basin in peninsular India, (**b**) geological map of the Kaladgi basin (modified after Mukherjee et al. 2016). Study area is shown with a rectangular outline. The northern and south-central sectors are distinguished on the basis of association of structural elements, their distribution and interrelationships (see text and figure 2).

Jayaprakash 2007) (figure 2). The deformational architecture of the basin and the structural details of the deformed Mesoproterozoic cover rocks have been comprehensively documented recently and explained in terms of basement–cover structural relationships and the origin of deformation of the cover (Mukherjee et al. 2016). On the basis of type, geometry, distribution, association of structural elements, variation and relative chronology of development, the deformation structures of the Mesoproterozoic sedimentary cover rocks of the basin can be grouped to define an extensional domain in the northern sectors and a contractional domain in the south-central sectors of the basin (Mukherjee et al. 2016) (figure 2). The extensional domain is characterised by development of a gently dipping (10°–15° due south) homocline that is affected at places by normal faults, tensile and hybrid joints and contain widely separated segments of the cover that are apparently extensional tear-apart of the cover across strike (Mukherjee et al. 2016). In the south-central sectors of the basin, an association of WNW–ESE trending, both northerly and southerly verging, asymmetric-to-overturned, plane non-cylindrical, gently plunging folds with axial planar cleavages, E–W trending thrusts and N–S trending strike-slip faults, together define the contractional domain. Distribution, variation and interrelationship of structural elements in the cover rocks reveal that the extensional and contractional domains lie adjacently (figure 2), spatially linked and are related to a single deformation event of the cover. The orientation of the structural grain of the Mesoproterozoic Bagalkot Group is E–W to WNW–ESE.

The basement cratonic assemblage consisting of the peninsular gneisses and the HSB have together undergone the multistage deformation with a structural grain of NW–SE. The Closepet granite is relatively undeformed. The strong contrast in the structural anatomy of the basement and the Mesoproterozoic sedimentary cover indicates that (i) the basement remained unaffected during the deformation of the cover and (ii) the deformation of the cover originated by a southerly directed

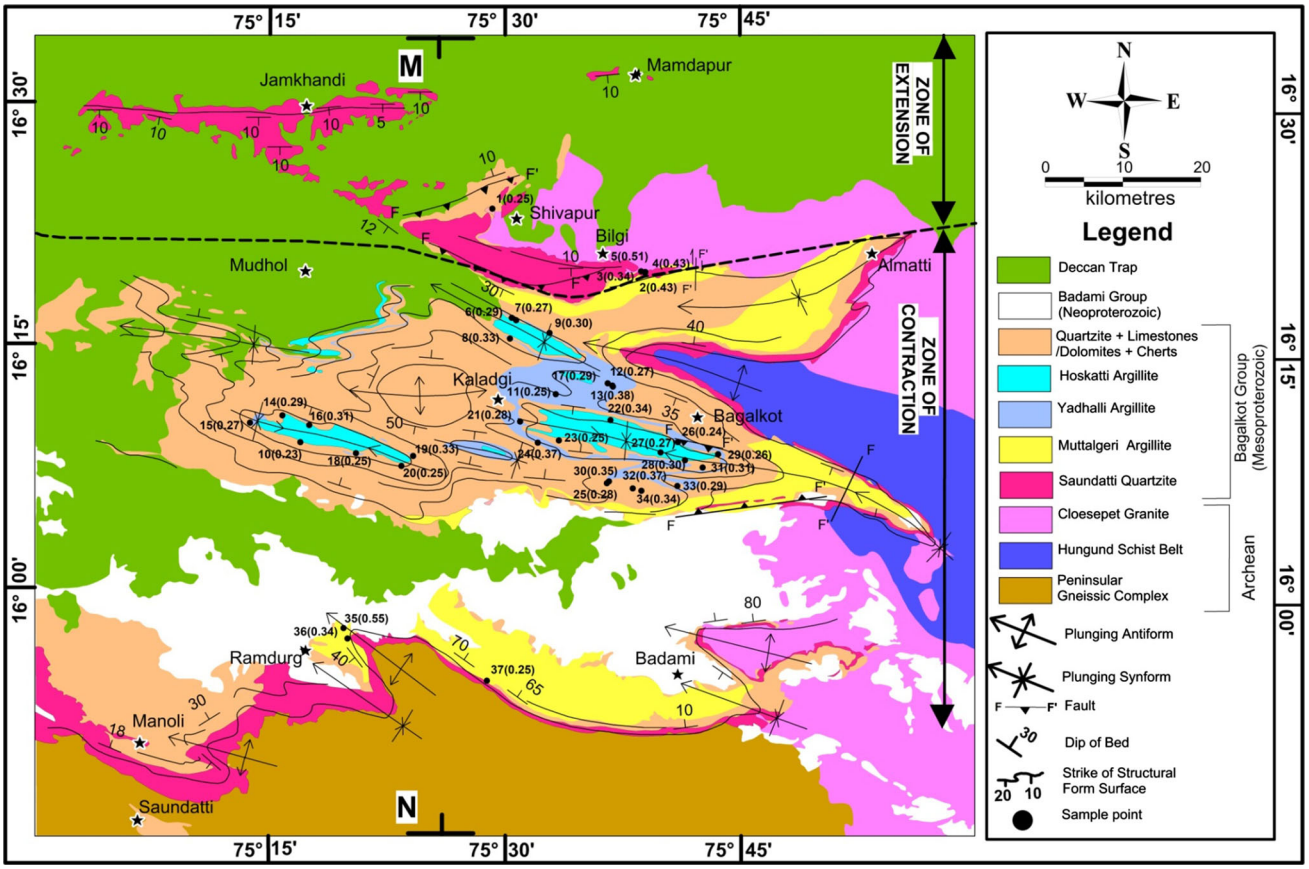

Figure 2. Geological map of the study area showing major structural elements and their distributions. The northern and south-central sectors shown in figure 1 are characterised by association and interrelationship of structural elements that define an extensional and contractional zone, respectively (for details see text). Location of sample points (filled circles) for this work is also indicated. Against each sample point, number without parenthesis indicates sample number and number within parenthesis denote illite crystallinity (IC) index value.

gravity gliding of the cover over the basement along the basement–cover contact (unconformity) that served as a surface of detachment (Mukherjee 2013, 2015; Mukherjee et al. 2015, 2016). The gravity gliding of the cover rocks produced an updip extensional zone and a downdip contractional zone as described above.

Overlying the deformed Mesoproterozoic cover rocks of the basin is the Neoproterozoic Badami Group in the southern and western parts of the basin. They represent shallow marine deposits (Sathyanarayan 1994) with fluvial components (Saha et al. 2016) and are composed of siliciclastics and carbonates (table 1). The Neoproterozoic Badami Group of rocks is undeformed, in general.

3. Methodology

3.1 *Sample collection*

Argillite mudrock samples were collected from north to south of the basin with an E–W spread along the central sectors of the basin. The sample collection was avoided in areas where there is evidence of post-deformational heating, e.g., veins, dykes, etc. The samples were collected principally from four stratigraphic units. These are (i) Ramdurg Formation (basal unit), containing argillite interbeds within Saundatti Quartzites; (ii) Yargatti Formation (intermediate lower unit), containing Muttalgeri argillite; (iii) Yadahalli Formation, (intermediate upper unit), containing Yadahalli argillites; and (iv) Hoskatti Formation (upper unit), containing Hoskatti argillites. Although stratigraphically they have an older–younger relationship, the samples themselves are spatially distributed (figure 2) and at no single location in the study area it was possible to collect samples along a vertical profile covering all the stratigraphic levels.

3.2 *Sample preparation*

IC values can be affected by several sample preparation factors (e.g., Kisch and Frey 1987;

Table 1. *Stratigraphy of the Kaladgi basin (modified after Jayaprakash 2007).*

Group	Sub-group	Formation	Member	Thickness (m)
Kaladgi super-group				
Badami (Neoproterozoic)		Katageri	Konkankoppa Limestone	85
			Halkurki Shale	67
			BelikhindiArenite	39
		..... *Sharp contact*		
		Kerur	Halgeri Shale	3
			Cave Temple Arenite	89
			Kendur Conglomerate	3
	..... *Angular unconformity*			
Bagalkot (Mesoproterozoic)	Simikeri	Hoskatti	Hoskatti Argillite	695
		..... *Transitional contact*		
		Arlikatti	Lakshanhatti Dolomite	87
			Kerkalmatti ferruginous member	42
			Neralkeri Chert	39
			Govindkoppa Argillite	80
		..... *Transitional contact*		
		Kundargi	Muchkundi Quartzite	182
			Bevinmatti Conglomerate	15
	..... *Disconformity*			
	Lokapur	Yadahalli	Yadahalli Argilite	58
		..... *Transitional contact*		
		Muddapur	Bamanbudni Dolomite	402
			Petlur Limestone	121
			Jalikatti Argillite	43
		..... *Sharp contact*		
		Yendigere	Nagnapur Dolomite	93
			Chikkashellikere	883
			Limestone Hebbal Argilite	166
		..... *Transitional contact*		
		Yargatti	Chitrabhanukot Dolomite	218
			Muttalgeri Argillite	502
		..... *Sharp contact*		
		Malprabha	Mahakut Chert	133
			Manoli Argillite	61
		..... *Transitional contact*		
		Ramdurg	Saundatti Quarzite	383
			Salgundi Conglomerate	31
Non-conformity/angular unconformity				
Basement rocks (Archaean)	Granitoids, Gneisses and Metasediments			

Kisch 1991; Krumm and Buggisch 1991; Warr and Rice 1994). Therefore, in studies that compare IC values, it is important to prepare samples uniformly. In the present work, the samples were prepared following the procedure by Meere (1995). Samples were brushed, rinsed and dried. Approximately 100 g of sample was disaggregated and powdered in an agate mortar to pass 0.2 mm sieve. The 5 g of powder was transferred to a 250 ml Erlenmeyer flask containing 50 ml 6% H_2O_2 and was placed in an ultrasonic bath for 30 min. About 5 ml of 1(N) HCl was added and the flask was put into a 70°C bath for 30 min. The suspensions were subsequently washed with distilled water until pH was neutral. This treatment was necessary to remove the calcium carbonate and organic matter present if any. The suspension is sieved wet to separate the fraction >50 μm. The suspension was transferred to a 20 cm high sedimentation cylinder, stirred well and after 70 min the upper 15 cm (containing <6 μm) was pipetted out. The process was repeated. The <6 μm fraction was

transferred to a 30 cm high sedimentation cylinder, stirred well and was allowed to settle for 17 h and 30 min. Then the upper 25 cm of liquid that contains <2 μm clay fraction was pipetted out. The process was repeated. The <2 μm size fraction was concentrated in a centrifuge.

The suspension containing <2 μm size fraction is freeze dried. For preparation of oriented specimens, 0.02 g of dry fraction was diluted with 0.50 ml of water and the suspension was put on a glass slide and was allowed to settle and the water evaporates under room temperature.

3.3 *XRD analysis*

XRD technique is used to identify the crystalline phases present in the samples. The XRD patterns of these samples were recorded in X'Pert Pro MPD diffractometer (PANalytical, Almelo, the Netherlands) using monochromator, operating at 40 kV and 30 mA using CuK_α radiation, with step size of 0.05°(2θ) and step time 50 s from 5° to 80° for these samples, in the XRD laboratory of Central Glass and Ceramic Research Institute (CGCRI), Kolkata, India. IC index values of the samples were determined by estimating the FWHM using X'Pert HighScore Plus software (PANalytical). Some samples were treated with ethylene glycol (EG) to evaluate the presence of expandable clays but in general EG treatment produced no measurable effects on XRD results.

Interlaboratory standardisation of XRD analysis results for reliable global comparisons between similar and contrasting geological environments had been strongly recommended by Warr and Rice (1994). They proposed a calibration approach to the standardisation of data using rock chip standards SWI, SW2, SW4 and SW6 and a muscovite flake (MF1) (all provided by Warr and Rice 1994), which allowed datasets produced by different research groups to be directly and quantitatively compared. The method involves preparation of the four international standards in the same way as other samples are prepared and performing XRD analysis on them under same instrumental settings in the laboratory. The measured values are then plotted against the calibrated values of the standards provided by Warr and Rice (1994) and a line of fit (calibration curve) is obtained that relates measured FWHM in any laboratory with the calibrated FWHM equivalent of Warr and Rice (1994) and are, therefore, globally comparable. Warr and Rice (1994) referred to their calibrated FWHM values of the four rock chip standards and a muscovite flake as crystallinity index standards (CIS) and when the measured FWHM values of samples in any laboratory is expressed in the FWHM equivalent of Warr and Rice (1994), by using the calibration curve as explained above, then it is referred to as IC_{CIS}. Warr and Rice (1994) also stated that as per their CIS scales the lower and upper boundaries of anchizone metamorphism are 0.42°$\Delta 2\theta$ and 0.25°$\Delta 2\theta$, respectively, and is same as the limits originally proposed by Kübler (1967). The CIS of Warr and Rice (1994) has been widely recognised as standard reference and IC studies worldwide are reported in terms of the CIS scales (see references in section 1).

The argillite samples of the Kaladgi basin were prepared and analysed in two batches according to their availability from the field and availability of time slots for analysis in the XRD laboratory of the CGCRI, India. Accordingly, the four rock chip standards for calibration provided by Warr and Rice (1994) were also prepared in two batches. The 'as measured' raw FWHM values of the standards SW1, SW2, SW4, SW6 and MF1 of Warr and Rice (1994), for the two batches, i.e., Batch-1 and Batch-2 samples are provided in table 2.

Using these measured FWHM values for the standards against the calibrated FWHM values of the standards provided by Warr and Rice (1994), the calibration equation for the two batches is as follows: for Batch-1 samples, the equation of calibration is $IC_{CIS} = 1.16 \times IC_{measured} + 0.0559 (R^2 = 0.984)$. For Batch-2 samples, the equation of calibration is $IC_{CIS} = 1.664 \times IC_{measured} - 0.0001 (R^2 = 0.951)$. The measured FWHM and also the calibrated FWHM (IC_{CIS}) of the Batch-1 and Batch-2 samples are given in table 3.

In a critical review of the CIS scales of Warr and Rice (1994) and Kisch et al. (2004), from their own evaluation of CIS and from similar evaluation from several laboratories worldwide, demonstrated that the anchizonal limits of the CIS of Warr and Rice (1994) differ considerably from that originally stated by Kübler (1967) for defining anchizone. Kisch et al. (2004) showed that Kubler's original anchizonal limits 0.42°$\Delta 2\theta$ – 0.25°$\Delta 2\theta$, although claimed to be similar in their CIS scales by Warr and Rice (1994), actually correspond to 0.49°$\Delta 2\theta$ – 0.295°$\Delta 2\theta$ of the CIS scales and is relatively broader than the Kubler equivalent. Following this, Warr and Mählmann (2015) redefined the CIS

Table 2. *FWHM values of the 10-Å basal reflections of illite-muscovite on Warr and Rice's (1994) CIS as measured in various laboratories.*

Sample no.	CIS (as calibrated by Warr and Rice 1994)	Warr (as measured)*	Kisch (as measured) (Kisch et al. 2004)	This work (as measured) during analysis of Batch-1 samples	This work (as measured) during analysis of Batch-2 samples)
SW1	0.630	0.57	0.480	0.496	0.369
SW2	0.470	0.38	0.385	0.339	0.260
SW4	0.380	0.31	0.269	0.302	0.254
SW6	0.250	0.20	0.170	0.183	0.174
MF1	0.110	0.06	0.079	0.047	0.066

'As measured' means raw uncalibrated data (values in $^\circ\Delta 2\theta$, CuK_α).
*As given by Warr in the CIS page of the very low-grade metamorphism (VLGM) website in Heidelberg (Kisch et al. 2004).

boundary limits of anchizone from $0.25^\circ\Delta 2\theta - 0.42^\circ\Delta 2\theta$ to corresponding $0.32^\circ\Delta 2\theta - 0.52^\circ\Delta 2\theta$. Kisch et al. (2004) also recommended that any IC data determined in the CIS scales should be reported in terms of Kisch or Kubler equivalent. Therefore, in the present work, the IC_{CIS} obtained from the samples of the Kaladgi basin by calibration using standards of Warr and Rice (1994) is converted to the corresponding Kubler equivalent (IC_{Kubler}) using the equation-4b and equation-6 of Kisch et al. (2004). The steps are as follows:

Step 1: $IC_{<\text{Warr, Heidelberg, equiv}>} = (IC_{CIS} - 0.051 - 958)/1.039613$ (from equation 6 of Kisch et al. 2004)
Step 2: $IC_{<\text{Kisch, Beer–Sheva equiv}>} = (IC_{<\text{Warr, Heidelberg, equiv}>} + 0.0207)/1.17$ (from equation 4b of Kisch et al. 2004).
Step 3: $IC_{<\text{Kubler}>} = IC_{<\text{Kisch, Beer–Sheva equiv}>} + 0.04^\circ\Delta 2\theta$ (Kisch 1980, 1990).

The IC_{Kubler}, thus, determined represents the Kubler equivalent of the IC_{CIS}. The IC_{Kubler} so obtained is hereafter referred to as the IC index.

4. Results

The clay mineral phases identified by XRD technique are Illite, kaolinite and chlorite (clinochore) and occur in samples that also contain quartz (figure 3). Two samples contain muscovite. The IC index was determined in 37 oriented specimens, by measurements from well-defined peaks of the illite 10-Å reflection in the $<2\,\mu$m size. After calibration of measurements using the approach by Warr and Rice (1994) and converting it to Kubler equivalent, the IC index so obtained is found to range in the analysed samples from $0.24^\circ\Delta 2\theta$ to $0.54^\circ\Delta 2\theta$ (table 3).

The distribution of the IC index values in the study area is shown in figure 2 along with the form surface of the map scale deformation structures. Isocryst contour map is constructed from the distribution of the IC index values in the basin and is illustrated in figure 4.

5. Discussion

5.1 *Variation of IC index and its controlling factors along and across the basin*

From the distribution of IC index data in the basin (figure 2) and its magnitude with distance from the

Table 3. *Measured FWHM, calibrated FWHM (IC_{CIS}) using CIS of Warr and Rice (1994) (table 2 of this work) and Kubler equivalent FWHM (IC_{Kubler}) of the 10-Å basal reflection of the Illite-muscovite in XRD analysis of the argillites of the Kaladgi Basin.*

Sample no.	Sample code	Stratigraphic identity	Northing	Easting	FWHM (measured)	IC_{CIS}	IC_{Kubler}
1*	22D/7(2014)	Saundatti Quartzite	16.3936111	75.48639	0.1973667	0.28	0.25
2†	13JN/7(2011)	Muttalgeri Argillite	16.3286111	75.64917	0.307	0.51	0.43
3†	9 OC/1(2013)	Saundatti Quartzite	16.3294444	75.64472	0.24	0.40	0.34
4†	13JN/5(2011)	Muttalgeri Argillite	16.3286111	75.64889	0.3053	0.51	0.43
5†	13JN/6(2011)	Muttalgeri Argillite	16.3283333	75.64861	0.36	0.60	0.51
6†	7OC/8(2013)	Yadahalli Argillite	16.2816667	75.50694	0.201	0.33	0.29
7†	7 OC/4(2013)	Hoskatti Argillite	16.2791667	75.51167	0.1877	0.31	0.27
8†	15D/4(2013)	Yadahalli Argillite	16.2602778	75.505	0.2301	0.38	0.33
9†	14D/1 (2013)	Yadahalli Argillite	16.2661111	75.54722	0.2093	0.35	0.30
10†	31J/4(2014)	Hoskatti Argillite	16.1541667	75.28194	0.1605	0.27	0.23
11*	14J/4(2015)	Yadahalli Argillite	16.2033333	75.55389	0.1985667	0.29	0.25
12†	3J/2(2013)	Yadahalli Argillite	16.2122222	75.61417	0.1878	0.31	0.27
13†	4 M/5(2011)	Yadahalli Argillite	16.2111111	75.61472	0.269	0.45	0.38
14†	21D/7 (2013)	Hoskatti Argillite	16.1816667	75.26278	0.2001	0.33	0.29
15†	23D/3 (2013)	Yadahalli Argillite	16.1741667	75.22833	0.1847	0.31	0.27
16†	26J/9(2014)	Hoskatti Argillite	16.1716667	75.29139	0.2167	0.36	0.31
17†	3J/4(2013)	Yadahalli Argillite	16.2144444	75.60917	0.2042	0.34	0.29
18†	17D/4(2013)	Yadahalli Argillite	16.1427778	75.34111	0.1728	0.29	0.25
19†	6 OC/7(2013)	Yadahalli Argillite	16.14	75.40194	0.2275	0.38	0.33
20†	20D/3 (2013)	Yadahalli Argillite	16.1297222	75.38944	0.1713	0.28	0.25
21†	19JN/5(2011)	Yadahalli Argillite	16.1752778	75.51583	0.1909	0.32	0.28
22†	3J/1(2013)	Hoskatti Argillite	16.1766667	75.61222	0.24	0.40	0.34
23†	17JN/3(2012)	Yadahalli Argillite	16.1558333	75.55722	0.1701	0.28	0.25
24†	5J/6(2013)	Yadahalli Argillite	16.1536111	75.53472	0.259	0.43	0.37
25†	5J/4B(2013)	Yadahalli Argillite	16.1119444	75.60833	0.1953	0.32	0.28
26†	3 M/7(2011)	Yadahalli Argillite	16.1541667	75.68389	0.1678	0.28	0.24
27†	5 M/8(2011)	Hoskatti Argillite	16.1436111	75.66556	0.1894	0.31	0.27
28†	5 M/7(2011)	Hoskatti Argillite	16.1355556	75.69139	0.2118	0.35	0.30
29†	2J/3(2011)	Hoskatti Argillite	16.1416667	75.72667	0.1761	0.29	0.26
30†	5J/3(2013)	Yadahalli Argillite	16.1138889	75.61056	0.2416	0.40	0.35
31†	28F/5(2011)	Hoskatti Argillite	16.1280556	75.71028	0.2161	0.36	0.31
32†	5 OC/6	Yadahalli Argillite	16.1066667	75.63583	0.2602	0.43	0.37
33†	13JN/3(2012)	Hoskatti Argillite	16.1091667	75.68333	0.2042	0.34	0.29
34†	15JN/2	Yadahalli Argillite	16.1041667	75.645	0.24	0.40	0.34
35*	23D/1(2014)	Muttalgeri Argillite	15.9658333	75.3292	0.507933	0.64	0.55
36*	23D/3(2014)	Muttalgeri Argillite	15.9525	75.34194	0.2888	0.39	0.34
37*	13JN/3A(2015)	Muttalgeri Argillite	15.9094444	75.48056	0.20303	0.29	0.25

*Batch-1 samples: calibration equation is $IC_{CIS} = 1.16 \times IC_{measured} + 0.0559 (R^2 = 0.984)$.

†Batch-2 samples: calibration equation is $IC_{CIS} = 1.664 \times IC_{measured} - 0.0001 (R^2 = 0.951)$.

northern boundary of the study area (figure 5), it is evident that IC index values vary both along and across the basin trend. In the northern sectors where there is extensional deformation, the IC index values range between 0.25°$\Delta 2\theta$ near Shivapur (figure 2) and 0.51°$\Delta 2\theta$ near Bilgi (figure 2). In the south-central sector in the zone of contraction (figure 2), the IC index values range between 0.24°$\Delta 2\theta$ and 0.38°$\Delta 2\theta$. At the southern boundary of the basin, the IC values range between 0.24°$\Delta 2\theta$ and 0.54°$\Delta 2\theta$.

Illite-smectite-to-illite and illite-to-muscovite transitions are related to sub-greenschist facies prograde metamorphism, i.e., anchizone metamorphism and both involve narrowing of 10-Å XRD peak (correspondingly less IC index value) with progressively higher metamorphic conditions (Merriman and Frey 1999). The anchizone bounded

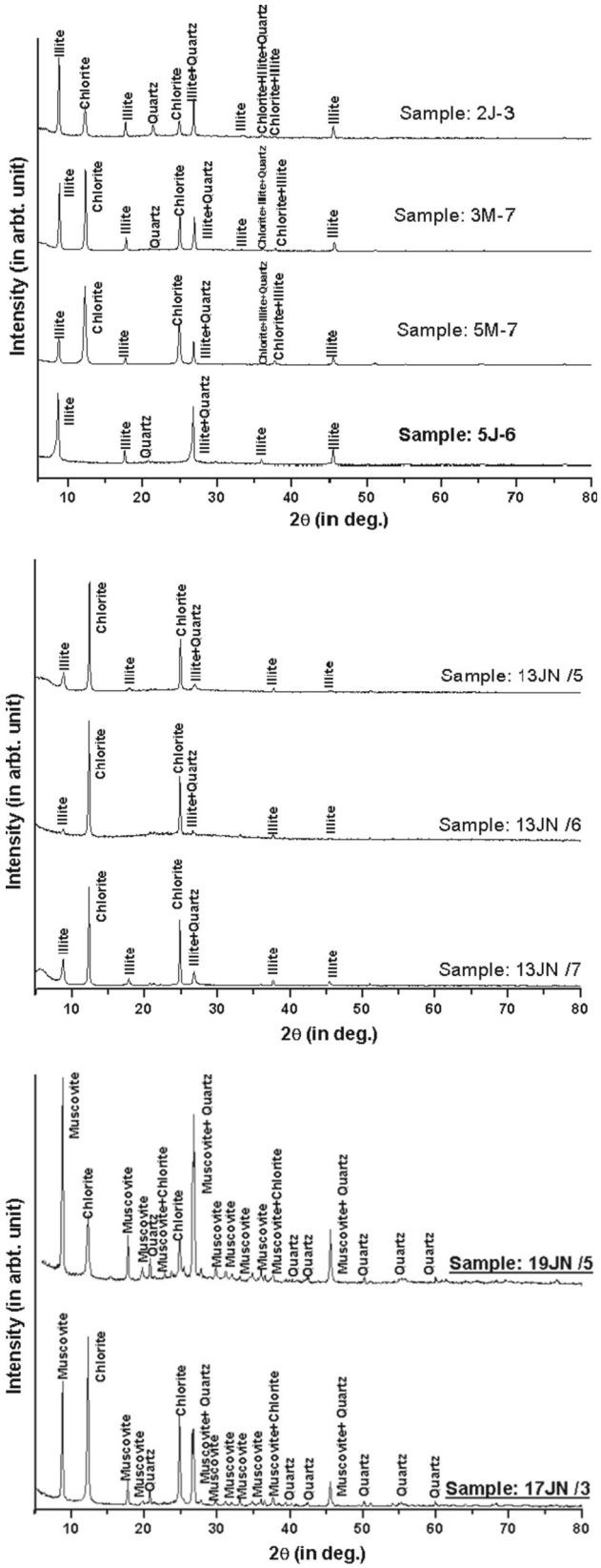

Figure 3. X-ray diffraction patterns of representative samples from the study area. Sample codes (e.g., 2J/3, 3 M/7, etc.) can be correlated with sample numbers from table 2 and their location in the study area can be found out from figure 2.

by 0.42°$\Delta 2\theta$ and 0.25°$\Delta 2\theta$ (Kübler 1967) is further divided into low and high zones (Merriman and Frey 1999). IC index values from 0.30°$\Delta 2\theta$ to 0.42°$\Delta 2\theta$ correspond to low anchizone, from 0.25°$\Delta 2\theta$ to 0.30°$\Delta 2\theta$ is high anchizone (figure 5). The dominant factor controlling the increase in IC index value is temperature although many other factors have been cited including fluid pressure, stress, lithology, crystal chemistry, mineralogy and time (Frey 1987). Deformation associated strain energy can also be important in aggradation of IC index values (Roberts and Merriman 1985; Merriman et al. 1990; Roberts et al. 1990, 1996). The temperature range from diagenetic to beginning of epizone is 100–300°C (Merriman and Frey 1999; Merriman and Peacor 1999). In the present study, the effect of lithology is minimised by using fine-grained argillaceous mudrock samples and the effect of time is minimised by selecting all specimens from the Mesoproterozoic age. The IC index values in the Kaladgi basin, therefore, correspond to a broad metamorphic grade from deep diagenetic to beginning of epizone spanning over a temperature range of ∼180 to 300°C (figure 5).

Across the basin, the IC index data are projected on a north–south oriented line MN (figure 2) and are plotted against distance (in km) from northern boundary of the map considering all stratigraphic units together (figure 5) and individually (figure 6) as well. The factors that might control such a distribution of IC index in the basin are a combined effect of subsidence and deformation.

When individual stratigraphic units are considered (figure 6), it is observed that IC index varies in the range 0.24°$\Delta 2\theta$–0.34°$\Delta 2\theta$ for Hoskatti argillites (figure 6a) and in the range of 0.24° $\Delta 2\theta$–0.38°$\Delta 2\theta$ for Yadahalli argillites (figure 6b) and none of these argillites show any trend of increase or decrease of IC index from north to south. For Muttalgeri argillites, the IC index varies in the range of 0.25°$\Delta 2\theta$–0.54°$\Delta 2\theta$ (figure 6c) and shows a mild decrease from north to south. The IC index of the argillites interbedded with Saundatti quartzites ranges from 0.24°$\Delta 2\theta$ to 0.34°$\Delta 2\theta$ (figure 6d). The factors that might control such a distribution and variation of IC index in the basin are variable subsidence, deformation patterns and a combination of subsidence and deformation.

In the northern sector (zone of extension), the dominant controlling factor would be subsidence since layer parallel contractional deformation is

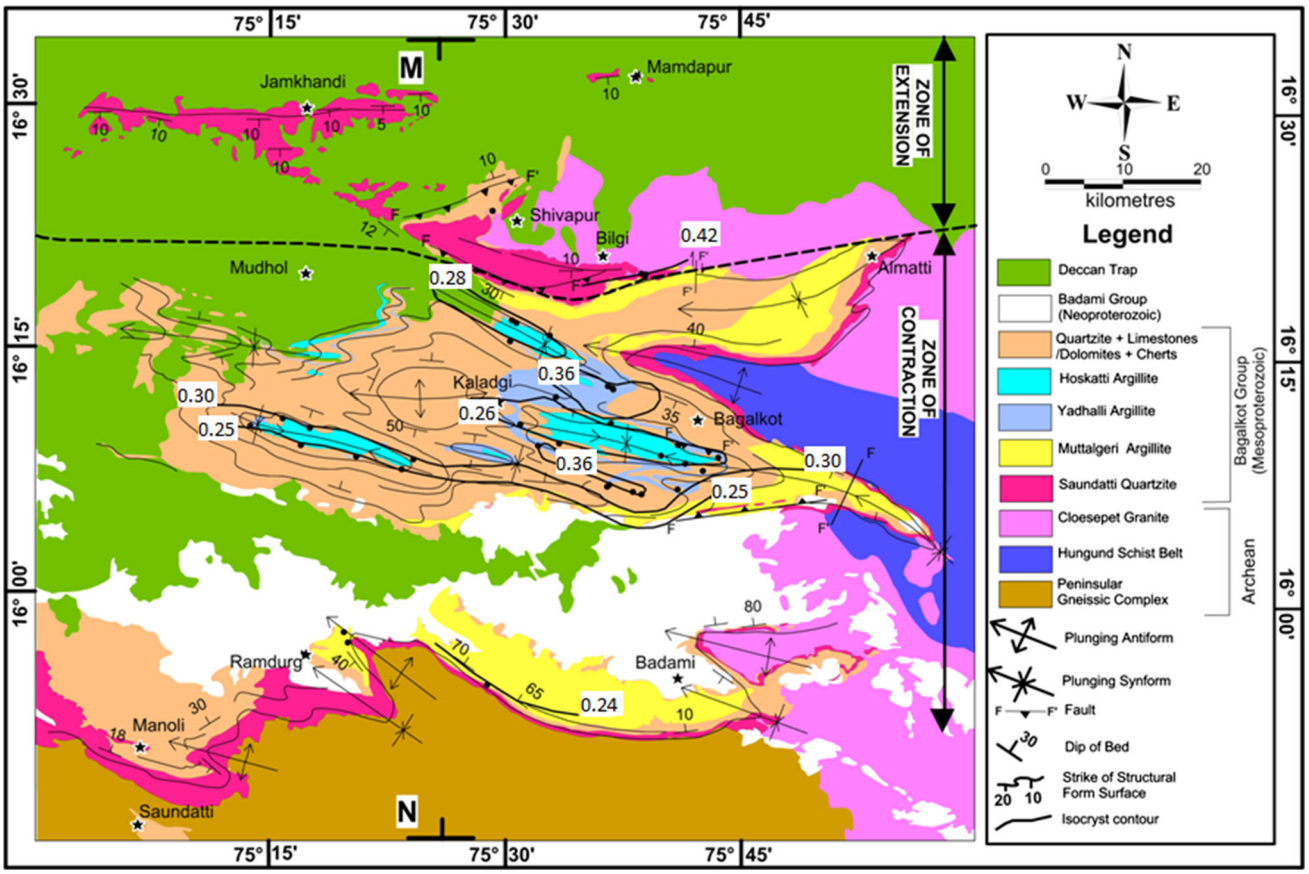

Figure 4. Isocryst contours drawn on the geological map of the study area. Note that the contours closely match with the map-scale synforms and antiforms.

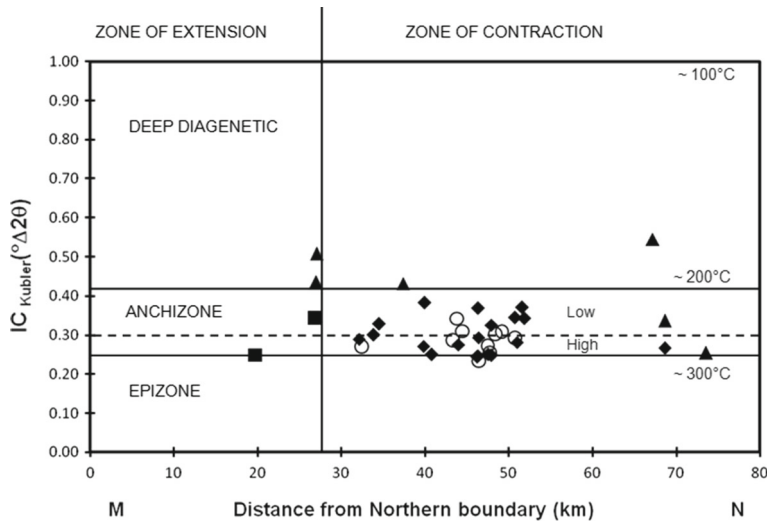

Figure 5. Synoptic plot of IC index versus distance from the northern boundary of the study area. All data were projected on MN (see figure 2) to indicate the variation in IC index values from north (M) to south (N). Open circles represent Hoskatti argillite, filled diamonds represent Yadahalli argillite, filled triangles represent Muttalgeri argillite and filled squares represent argillites interbedded with Saundatti Quartzites. Note that the IC index corresponds to the deep-diagenetic to high anchizone to beginning of epizone. Thermal boundaries are according to Merriman and Frey (1999).

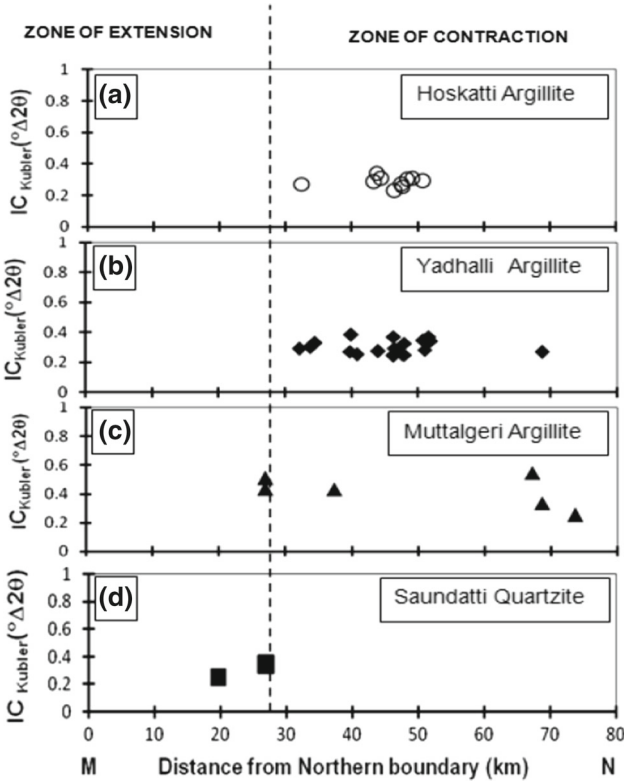

Figure 6. Plot of IC index versus distance from northern boundary for individual stratigraphic units. All data were projected on MN (see figure 2) to indicate the variation in IC index values from north (M) to south (N). IC index of (**a**) Hoskatti argillites (Hoskatti Formation) with range $0.24°\Delta 2\theta$–$0.34°\Delta 2\theta$, (**b**) Yadahalli argillites (Yadahalli Formation) with range $0.24°\Delta 2\theta$–$0.38°\Delta 2\theta$, (**c**) Muttalgeri argillite (Yargatti Formation) with range $0.25°\Delta 2\theta$–$0.54°\Delta 2\theta$ and (**d**) argillites interbedded with Saundatti quartzites with range $0.25°\Delta 2\theta$–$0.34°\Delta 2\theta$.

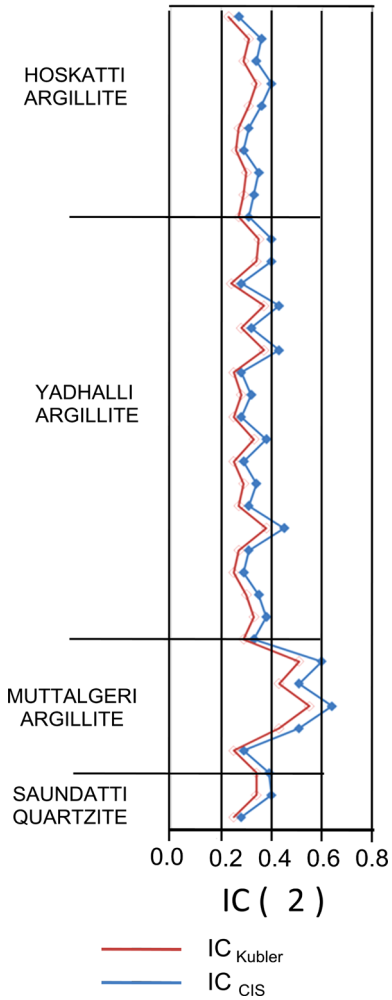

Figure 7. Stratigraphic distribution of IC index data. Relatively lower IC index and therefore higher metamorphic grade of the younger stratigraphic unit (e.g., Hoskatti Argillite) compared with the lower units indicate that burial was not the controlling factor for the variation of IC index. Both IC_{CIS} and IC_{Kubler} values are shown.

absent. From the IC index values, the burial depth is apparently relatively shallow around Bilgi but relatively deep near Shivapur. The deeper burial depth near Shivapur is interpreted as a basinal low with additional depth in the hanging wall due to extensional fault (figure 2).

In the contraction zone, at a distance of 40 km from the northern boundary of the study area (figure 6), it can be observed that IC index from the same stratigraphic unit, e.g., Yadahalli argillite (figure 6b) have relatively high and low index values. Similarly at ∼48 km distance from the northern boundary (figure 6), both Yadahalli and Hoskatti argillites possess within themselves, relatively high and low IC index values. The fact that within the same stratigraphic member, samples in the basin that occur at the same distance from the northern boundary possess relatively high and low IC index, and therefore, it indicates a variation of IC index along the basin trend and possibly controlled by variable depths of subsidence of the sedimentary cover at certain locations. An important consequence of such variation in depths of subsidence is the development of basinal highs and lows along and across the basin trend. In the zone of contraction, in the south-central sector, the dominant controlling factor is a combination of layer parallel contractional deformation and variable depth of subsidence. This is evident from two observations viz. (i) The isocryst contour map closely matches with the map-scale folds (figure 5). (ii) Lower IC index corresponds to the elevated temperatures in the stratigraphically younger Hoskatti argillites of Hoskatti Formation compared with relatively older Muttalgeri argillites of Yargatti Formation (figures 6, 7). The latter

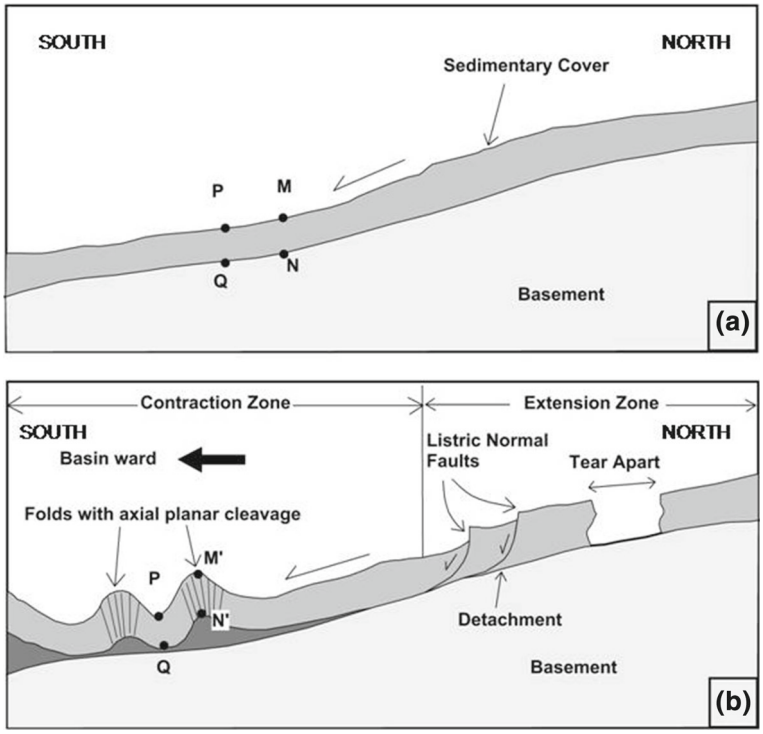

Figure 8. Preservation of subsidence depth in synform, during deformation of a sedimentary layer due to gravity gliding. (**a**) Points P, Q, M and N occur on the undeformed sedimentary cover lying over a basement. (**b**) After basinward gravity gliding of the layer, points M and N on the undeformed layer now take up positions M′ and N′ on the antiform hinge and are, therefore, at crustal depths shallower than their original depth. Points P and Q on the undeformed layer retain their original subsidence depth after deformation since they occupy the hinges of synform.

cannot be explained by a simple burial model in a 'layer cake' stratigraphic set up. Furthermore, the similarity in metamorphic grade between the older and younger units (figures 6, 7) suggests that burial was not the main control that caused IC index variation in the south-central sectors of the basin. Aggradation of IC index due to layer parallel contractional deformation involving all stratigraphic units simultaneously would produce similar metamorphic grades. The older Muttalgeri argillites, whose temperatures were relatively low (high IC index) compared with the young Hoskatti argillites, were collected from the zone of extension in the northern sector and the Hoskatti argillites were from the contractional zone corresponding to the deformed south-central sectors of the basin, which bear prominent development of penetrative cleavage that are axial planar to the map scale and mesoscale folds (Mukherjee et al. 2016). The same Muttalgeri argillites show a low IC index value along with the southern boundary of the basin in the contractional zone. An additional effect of variable subsidence depths is also evident in the contractional zone, from the fact that along the basin trend, IC index has variable values from the same stratigraphic units even though the structures are similar (figure 2). However, the precise determination of this additional effect of variation of subsidence depth in the zone of contraction on IC index values becomes challenging due to overprinting effect of deformation.

5.2 *Implication on crustal depth of subsidence and deformation*

An important question of research is: At what crustal depth the gravity gliding deformation has occurred? Is it different from the depth of subsidence? The crux of the problem lies in separating out the depths of deformation and subsidence where both have a control on IC index. For this we need an accurate thermometric input that is sensitive to both. Since IC index is mostly temperature dependent, the range of IC index from $0.54°\Delta 2\theta$ to $0.24°\Delta 2\theta$ corresponds to temperature range of ~180 to 300°C (figure 5).

In the northern sector, between Bilgi and Shivapur (figure 1), the IC index data range between $0.51°\Delta 2\theta$ and $0.25°\Delta 2\theta$, indicating a temperature range of ~180 to 300°C. Since this is the zone

of extension and the effect of layer parallel compressive deformation is nil, the depth range at which the corresponding temperature range exists, therefore, corresponds to subsidence depth. During the Mesoproterozoic the geothermal gradient was relatively steep and averaged to ∼35°C/km (Grambling 1981). Hence, the depth of subsidence is in the range of 5.14–8.57 km in the zone of extension. In the south-central sectors of the basin, the effects of contractional deformation and subsidence are combined. In a gravity-gliding deformation, the basement is not involved in the deformation of the cover and when the cover gets folded into antiforms and synforms in the contractional zone, the hinges of synforms, therefore, will essentially be at the same depth before and after deformation (figure 8) and would signify the original subsidence depth. From the isocryst contour map (figure 4), IC index values associated with synformal depressions range between $0.25°\Delta 2\theta$ and $0.30°\Delta 2\theta$, within a corresponding temperature range of ∼270 to 300°C. Considering the Mesoproterozoic mean geothermal gradient of ∼35°C/km (Grambling 1981), this would translate into a crustal depth range of 7.71–8.57 km corresponding to depths of both original subsidence and deformation. The remaining areas would signify the post-subsidence modified depth of cover due to contractional deformation.

6. Conclusion

1. The Mesoproterozoic Bagalkot Group of rocks of the Kaladgi basin that underwent deformation related to southward gravity gliding has been studied with reference to IC index (Kubler equivalent) and its distributions and variations along and across the basin.
2. The IC index range from $0.54°\Delta 2\theta$ to $0.24°\Delta 2\theta$ and indicates a deep diagenetic to high anchizone to beginning of epizone metamorphism within a temperature range of ∼180 to 300°C.
3. The dominant controlling factor on IC index values is temperature that results from crustal depth of the sample points. The depth of sample points results from a combination of subsidence and deformation. Assuming a Mesoproterozoic mean geothermal gradient of 35°C/km, the IC index values in the extensional zone of the deformed Mesoproterozoic cover (northern sector) imply a subsidence depth of 5.14–8.57 km. In the contractional zone (south-central sector), the IC index values imply a depth of subsidence and deformation in the range 7.71–8.57 km.

Acknowledgements

The research was funded by the Science and Engineering Research Board, Department of Science and Technology, Govt. of India, Project No. SR/S4/ES-516/2010, awarded to MKM at IIT (ISM), Dhanbad. KM acknowledges the financial support from Junior Research Fellowships awarded to him by IIT (ISM), Dhanbad. The authors gratefully acknowledge the critical comments and suggestions of two anonymous reviewers and Prof. Saibal Gupta who has significantly improved the paper. MKM conveys special thanks to Dr. Sagar Pal, Department of Applied Chemistry, IIT (ISM), Dhanbad, for his cooperation during the sample preparation.

References

Awan M A and Woodcock N H 1991 A white mica crystallinity study of the Berwyn Hills, North Wales; *J. Metamor. Geol.* **9** 765–773.

Essene E J and Peacor D R 1995 Clay mineral thermometry – A critical perspective; *Clay Clay Miner.* **43** 540–553.

Fitz-Díaz E, Camprubí A, Cienfuegos-Alvarado E, Morales-Puente P, Schleicher A M and Van der Pluijm B A 2014 Newly-formed illite preserves fluid sources during folding of shale and limestone rocks; an example from the Mexican Fold-Thrust Belt; *Earth Planet. Sci. Lett.* **391** 263–273.

Frey M 1987 Very low-grade metamorphism of clastic sedimentary rocks; In: *Low temperature metamorphism* (ed) Frey M, Chapman & Hall, New York, pp. 9–58.

Frey M 1988 Discontinuous inverse metamorphic zonation, Glarus Alps, Switzerland: Evidence from illite "crystallinity" data; *Schwei. Miner Petrograph. Mitt.* **68** 171–183.

Frey M, Teichmiiller M, Teichmtiller R, Mullis J, Kiinzi B, Breitschmid A, Gruner U and Schwizer B 1980 Very low-grade metamorphism in external parts of the Central Alps: Illite crystallinity, coal rank and fluid inclusion data; *Eclogae Geol. Helv.* **73** 173–203.

Fukuchi R, Fujimoto K, Kameda J, Hamahashi M, Yamaguchi A, Kimura G, Hamada Y, hashimoto Y, Kitamura Y and Saito S 2014 Changes in illite crystallinity within an ancient tectonic boundary thrust caused by thermal, mechanical and hydrothermal effects: An example from the Nobeoka Thrust, southwest Japan; *Earth Planets Space* **66** 116, https://doi.org/10.1186/1880-5981-66-116.

Grambling J A 1981 Pressures and temperatures in Precambrian Metamorphic rocks; *Earth Planet. Sci. Lett.* **53** 63–68.

Gutierrez-Alonso G and Nieto F 1996 White-mica 'crystallinity', finite strain and cleavage development across a

large Variscan structure, NW Spain; *J. Geol. Soc. London* **153** 287–299.

Hara H and Kurihara T 2010 Tectonic evolution of low-grade metamorphosed rocks of the Cretaceous Shimanto accretionary complex, Central Japan; *Tectonophysics* **485** 52–61.

Jaboyedoff M, Bussy F, Kübler B and Thélin P 2001 Illite "crystallinity" revisited; *Clay Clay Miner.* **49** 156–167.

Jayaprakash A V 2007 Purana Basins of Karnataka; *Mem. Geol. Surv. India* **129** 1–137.

Jayaprakash A V, Sundaram V, Hans S K and Mishra R N 1987 Geology of the Kaladgi–Badami Basin, Karnataka; *Mem. Geol. Soc. India* **6** 201–226.

Kale V S and Phansalkar V G 1991 Purana basins of Peninsular India: A review; *Basin Res.* **3** 1–36.

Kisch H J 1983 Mineralogy and petrology of burial diagenesis (burial metamorphism) and incipient metamorphism in clastic rocks; In: *Diagenesis in sediments and sedimentary rocks* (eds) Larsen G and Chilingar G V, Elsevier, Amsterdam **2** 289–493.

Kisch H J 1991 Illite crystallinity: Recommendations on sample preparation, X-ray diffraction settings, and interlaboratory samples; *J. Metamor. Geol.* **9** 665–670.

Kisch H J and Frey M 1987 Appendix: Effect of sample preparation on the measured 10A° peak width of illite (illite 'crystallinity'); In: *Low temperature metamorphism* (ed) Frey M, Chapman & Hall, New York, pp. 301–304.

Kisch H J, Arkai P and Brime C 2004 On the calibration of the illite Kübler index (illite 'crystallinity'); *Schweiz. Mineral. Petrogr. Mitt.* **84** 323–331.

Krumm S and Buggisch W 1991 Sample preparation effects on illite crystallinity measurement: Grain-size gradation and particle orientation; *J. Metamorp. Geol.* **9** 671–677.

Kübler B 1967 La cristallinité de l'illite et les zones tout á fait supérieures du métamorphisme; In: *Étages tectoniques, Colloque de Neuchátel 1966*, Edition de la Baconnière, Neuchátel, Switzerland, pp. 105–121.

Kübler B and Jaboyedoff M 2000 Illite crystallinity; *C. R. Acad. Sci. Paris* **331** 75–89.

Kulkarni K G and Borkar V D 1999 Trace fossils from the Kaladgi and Bhima Basis: A review. Abstract volume on fieldworkshop on integrated evaluation of the Kaladgi and Bhima Basins; *Geol. Soc. India*, pp. 37–39.

Lee YI and Ko H K 1997 Illite crystallinity and fluid inclusion analysis across a Paleozoic disconforrnity in central Korea; *Clay Clay Miner.* **45** 147–157.

Lee JI and Lee Y I 2001 Kübler 'illite crystallinity' index of the cretaceous Gyeongsang basin, Korea: Implications for basin evolution; *Clay Clay Miner.* **49** 36–43.

Mani, M S 1974 *Ecology and biostratigraphy in India*; Dr. W. Junk. B.V. Publishers, The Hague, 67p.

Meere P A 1995 Subgreenschist facies metamorphism from the Variscides of SW Ireland: An early syn-extensional peak thermal event; *J. Geol. Soc. London* **152** 511–521.

Merriman R J and Frey M 1999 Pattern of very low-grade metamorphism in metapelitic rocks; In: *Low-grade metamorphism* (eds) Frey M and Robinson D, Blackwell Science, Oxford, UK, pp. 61–107.

Merriman R J and Peacor D R 1999 Very low-grade metapelites: Mineralogy, microfabrics and measuring reaction progress; In: *Low-grade metamorphism* (eds) Frey M and Robinson D, Blackwell Science, Oxford, UK, pp. 10–60.

Merriman R J, Roberts B and Peacor D R 1990 A transmission electron microscope study of white mica crystallite size distribution in a mudstone to slate transitional sequence, North Wales, UK; *Contrib. Mineral Petrol.* **106** 27–40.

Moore D M and Reynolds R C 1997 *X-ray diffraction and the identification and analysis of clay minerals*; 2nd edn, Oxford University Press, New York, 378p.

Mukherjee M K 2003 Very low grade metamorphism vis-avis penetrative deformation in the Southern Nallamalai fold-fault belt, Cuddapah basin Andhra Pradesh; *J. Geol. Soc. India* **62** 535–548.

Mukherjee M K 2013 Contrasting deformation Geometry, Kinematics and Microstructures between the Basement and the Mesoproterozoic cover rocks of the Kaladgi Basin, South-western India: indications towards deformation of the cover by gravity gliding along a detached unconformity; In: *Proceedings of the international conference on deformation mechanism, rheology and tectonics (DRT)*, Leuven, Belgium, p. 53.

Mukherjee M K 2015 Basement-cover relations in the intracratonic Kaladgi basin, southwestern India: Deformational evidence of a Mesoproterozoic gravity gliding of the cover over the basement; In: *Riding the wave: GSA specialist group in tectonics and structural geology conference*, November 2015, Geol. Soc. Austral. Abs. no. 113 (eds) Siégel C, Verdel C and Rosenbaum G, pp. 104–105.

Mukherjee M K, Modak K and Das S 2015 Deformation scenario and metamorphism of the Mesoproterozoic cover rocks of the Kaladgi basin, southwestern India; In: *Proceedings of the* 4th *annual international conference on geological & earth sciences (GEOS 2015)*, October 2015, Singapore, Global Science and Technology Forum, pp. 50–61, https://doi.org/10.5176/2251-3353_GEOS15.42

Mukherjee M K, Das S and Modak K 2016 Basement-Cover structural relationships in the Kaladgi Basin, southwestern India: Indications towards a Mesoproterozoic gravity gliding of the cover along a detached unconformity; *Precamb. Res.* **281**, 495–520, https://doi.org/10.1016/j.precamres.2016.06.013-0310-9268.

Padmakumari V M, Sambasiva Rao V V and Srinivasan R 1998 Model Nd and Rb–Sr ages of shales of the Bagalkot Group, Kaladgi Supergroup, Karnataka; In: *Abstracts, National symposium on Late Quaternary geology and sea level changes*, Cochin University, Kochi, p. 70.

Patil S P, Pandey K and Kale V S 2018 Implications of new 40Ar/39Ar age of Mallapur intrusives on the chronology and evolution of the Kaladgi basin, Dharwar craton, India; *J. Earth Syst. Sci.* **127** 32, https://doi.org/10.1007/s12040-018-0940-5.

Pillai S 1997 Study of stromatolitic growth patterns and their implications with reference to the Vindhyanchal and Kaladgi Basins; Unpublished PhD Thesis, Pune University, Pune, India.

Pillai P S and Kale V S 2011 Seismites in the Lokapur Subgroup of the Proterozoic Kaladgi basin, south India: A testimony to synsedimentary tectonism; *Sedim. Geol.* **240** 1–13.

Rao S, Parthasarthy V V, Padmakumari V M and Srinivasan R 1999 Shales of the Proterozoic Bagalkot and Bhima

Groups, Southern India – A mineralogical and chemical appraisal. Abstract volume on Fieldworkshop on Integrated Evaluation of the Kaladgi and Bhima Basins; *Geol. Soc. India*, pp. 33–35.

Roberts B and Merriman R J 1985 The distinction between Caledonian burial and regional metamorphism in metapelites from North Wales: An analysis of isocryst patterns; *J. Geol. Soc. London* **142** 615–624.

Roberts B, Morrison C and Hirons S 1990 Low grade metamorphism of the Manx Group, Isle of Man: A comparative study of white mica 'crystallinity' techniques; *J. Geol. Soc. London* **147** 271–277.

Roberts B, Merriman R J, Hirons S R, Fletcher C T N and Wilson D 1996 Synchronous very low-grade metamorphism, contraction and inversion in the central part of the Welsh Lower Palaeozoic Basin; *J. Geol. Soc. London* **153** 277–285.

Ruiz G M H, Helg U, Negro F, Adatte T and Burkhard M 2008 Illite-crystallinity patterns in the anti-Atlas of Morocco; *Swiss J. Geosci.* **101** 387–395.

Saha D, Patranabis-Deb S and Collins A S 2016 Proterozoic stratigraphy of southern Indian cratons and global context; In: *Stratigraphy and timescales* (ed) Montenari M, Vol. **1,** pp. 1–59. https://doi.org/10.1016/bs.sats.2016.10.003.

Sathyanarayan S 1994 The Younger Proterozoic Badami Group, Northern Karnataka; In: '*Geo Karnataka*', MGD Centenary volume, pp. 227–233.

Sharma M and Pandey S K 2012 Stromatolites of the Kaladgi Basin, Karnataka, India: Systematics, biostratigraphy and age implications; *Palaeobotanist* **61** 103–121.

Verdel C, Niemi N and Van der Pluijm B A 2011 Variation in the illite to muscovite transition relate to metamorphic conditions and detrital muscovite content: Insights from the palaeozoic passive margin of the southwestern United States; *J. Geol.* **119** 419–437.

Warr L N and Mählmann R F 2015 Recommendations for Kübler Index Standardization; *Clay Miner.* **50** 283–286.

Warr L N and Rice A H N 1994 Interlaboratory standardization and calibration of clay mineral crystallinity and crystallite size data; *J. Metamor. Geol.* **12** 141–152.

Warr L N, Greiling R O and Zachrisson E 1996 Thrust-related very low grade metamorphism in the marginal part of an orogenic wedge, Scandinavian Caledonides; *Tectonics* **15** 1213–1229.

Wensink H and Klootwijk C T 1970 Palaeomagnetism of the Deccan Traps in the Western Ghats, near Poona (INDIA); *Tectonophysics* **11** 175–190.

Corresponding editor: Saibal Gupta